



Research Article

# Investigating the anti-cancer potential of sulfatase 1 and its underlying mechanism in non-small cell lung cancer

Bingling Zhang<sup>MM1</sup>, Daping Luo<sup>MB2</sup>, Lan Xiang<sup>MB3</sup>, Jun Chen<sup>MB1</sup>, Ting Fang<sup>MM4</sup>

<sup>1</sup>Department of Disease Control and Prevention, Zhangqiao Branch, Ningbo Ninth Hospital Medical Health Group, Ningbo, <sup>2</sup>Department of Prevention and Healthcare, Hongtang Branch, Ningbo Ninth Hospital Medical Health Group, Ningbo, <sup>3</sup>Department of Doctor-Patient Communication, The First Affiliated Hospital of Ningbo University, Ningbo, <sup>4</sup>Medical College, Ningbo University Health Science Center, Ningbo, China.



\*Corresponding author:

Ting Fang,  
Medical College, Ningbo  
University Health Science  
Center, Ningbo, China.

ningbozbb@163.com

Received: 24 May 2024

Accepted: 29 September 2024

Published: 23 November 2024

DOI

10.25259/Cytojournal\_71\_2024

Quick Response Code:



## ABSTRACT

**Objective:** Patients with non-small cell lung cancer (NSCLC) have poor prognoses. Sulfatase 1 (SULF1) is an extracellular neutral sulfatase and is involved in multiple physiological processes. Hence, this study investigated the function and possible mechanisms of SULF1 in NSCLC.

**Material and Methods:** Difference in SULF1 expression level between tumors and normal lung tissues was analyzed through bioinformatics and clinical sampling, and the effects of SULF1 expression on prognosis were investigated through Kaplan–Meier analysis. SULF1 level in NSCLC cells was modulated through small interfering ribonucleic acid interference. NSC228155, which is an epidermal growth factor receptor (EGFR)/mitogen-activated protein kinase (MAPK) signaling pathway agonist, was for handling NSCLC cells. SULF1 expression level was tested through quantitative reverse transcriptase real-time polymerase chain reaction. Cell proliferation, migration, and invasion were evaluated with cell counting kit-8, 5-ethynyl-2-deoxyuridine, and transwell assays, and the levels of epithelial-to-mesenchymal transition (EMT)- and EGFR/MAPK pathway-related proteins were detected through Western blot.

**Results:** Bioinformatics and clinical samples showed that NSCLC tumor tissues had elevated SULF1 expression levels relative to those of normal tissues ( $P < 0.05$ ). Patients with NSCLC and high SULF1 expression levels experienced poorer prognosis than those of low SULF1 expression levels ( $P < 0.05$ ). SULF1 knockdown repressed the malignant biological behavior, including proliferation, migration, and invasion, of the NSCLC cells ( $P < 0.05$ ). Mechanistically, SULF1 knockdown augmented E-cadherin level and abated N-cadherin and vimentin protein levels ( $P < 0.05$ ). These results confirmed that EMT was inhibited. In addition, the knockdown of SULF1 reduced the phosphorylation of EGFR, extracellular signal-regulated kinase, p38 MAPK and c-Jun N-terminal kinase, and NSC228155 partially reversed these changes, which were affected by SULF1 knockdown. Meanwhile, NSC228155 partially reversed the inhibition of EMT, migration, and invasion affected by SULF1 knockdown.

**Conclusion:** SULF1 knockdown inhibits the proliferation, migration, invasion, and EMT of NSCLC cells by inactivating EGFR/MAPK pathway.

**Keywords:** Sulfatase 1, Non-small cell lung cancer, Epidermal growth factor receptor, Mitogen-activated protein kinase, Epithelial-mesenchymal transition

## INTRODUCTION

Non-small cell lung cancer (NSCLC) accounts for approximately 80–85% of lung cancer cases.<sup>[1,2]</sup> In recent years, the diagnostic strategies and treatment methods of NSCLC have been continuously developed, but patients showed unfavorable prognoses, with low 5-year survival

rates.<sup>[3,4]</sup> Hence, further exploring functional genes related to the onset and advance of NSCLC is beneficial for NSCLC therapy.

Sulfatase 1 (SULF1) is one of extracellular sulfatases and functions in signal transduction, cell development, tumorigenesis, muscle regeneration, and immune regulation.<sup>[5]</sup> A study has shown that SULF1 is augmented in cervical cancer tissues and is prominently linked to its poor prognosis.<sup>[6]</sup> Moreover, a research has pointed out that SULF1 is carcinogenic in multiple malignant tumors and linked to poor survival,<sup>[7]</sup> but the role of SULF1 in NSCLC remains unclear.

As a member of the receptor tyrosine kinase ErbB family, epidermal growth factor receptor (EGFR) has a crucial function in physiological events. It usually mutates or is overexpressed in different cancer types and is a therapeutic target for a variety of clinical cancer.<sup>[8,9]</sup> Osimertinib is an EGFR-tyrosine kinase inhibitor and the standard therapy for patients with advanced NSCLC concomitant with EGFR mutation; its safety and efficacy have been confirmed.<sup>[10]</sup> EGFR exerts physiological functions through ligand binding. After combination, tyrosine residues in EGFR undergo dimerization and autophosphorylation, and EGFR activates downstream signaling through mitogen-activated protein kinase (MAPK) and phosphatidylinositol-3-kinase (PI3K) pathways, thereby regulating physiologic properties in tumor cells.<sup>[11]</sup> The EGFR/MAPK signaling pathway is a potential therapeutic target against NSCLC because of its contribution to cancer cell proliferation, angiogenesis, and metastasis.<sup>[12,13]</sup> Long non-coding ribonucleic acid nuclear-enriched abundant transcript 1 knockdown can inhibit MAPK signaling by modulating SULF1 in NSCLC cells.<sup>[14]</sup> However, the effects of SULF1 on the EGFR/MAPK signaling pathway and whether it is involved in the course of NSCLC have not been reported. Our research objective was to examine the effects and potential molecular mechanisms of SULF1 in NSCLC. The SULF1 expression in the tumor tissues was assessed, and the changes affected by SULF1 knockdown in NSCLC were evaluated *in vitro*. This study may assist in the exploration of potential therapeutic targets for NSCLC.

## MATERIAL AND METHODS

### Cell cultivation and small interfering RNA (siRNA) transfection

American Tissue Culture Collection (Manassas, VA, USA) provided the NSCLC cell lines: NCI-H1299 (CRL-5803) and HCC827 (CRL-2868) cells. Human normal lung epithelial cells BEAS-2B (TCH-C132), human normal lung epithelial cells, was obtained from Suzhou Haixing Biotechnology Co., Ltd. (Suzhou, China). Short tandem repeat profiling and mycoplasma testing were carried out before experiments. Dulbecco's modified Eagle's medium

(11885084) containing 10% fetal bovine serum (10099-141) and penicillin/streptomycin (15070063) were used for cell cultivation. Reagents for cell cultivation were sourced from Gibco (Thermo Fisher Scientific, Waltham, MA, USA). The temperature and carbon dioxide(CO<sub>2</sub>) supply of the incubator was set at 37°C and 5%, respectively.

siRNA was designed and synthesized by Guangzhou Ruibo Biotechnology Co., Ltd. (Guangzhou, China), and sequences were as follows: Negative control (si-NC; 5'-AUGCUGATCAGUGUCGATU-3') and siRNA SULF1 (si-SULF1; 5'-CGGGAAGTATGTGCACAATCACA-3'). Lipofectamine 3000 (L3000015, Thermo Fisher Scientific, Inc., Waltham, MA, USA) was used in transfecting NSCLC cells with si-NC or si-SULF1. After 48 h of transfection, subsequent experiments were undertaken using the collected cells. NSC228155 (100 μM, HY-101084, MCE, Shanghai, China), an EGFR/MAPK pathway agonist, was used for processing NCI-H1299 cells.

### Quantitative real-time polymerase chain reaction (qRT-PCR)

Trizol (Sigma-Aldrich, T9424, Saint Louis, MO, USA) was used for total RNA extraction. Complementary deoxyribonucleic acid synthesis was conducted in accordance with the instructions of HiScript III RT SuperMix (R323-01, Vazyme Biotech Co., Ltd., Nanjing, China). A reaction system for fluorescence quantitative polymerase chain reaction (qPCR) detection was established using an AceQ qPCR Synergy Brands Green master kit (Vazyme Biotech Co. Ltd., Q111-02, Nanjing, China). The reaction procedures were as follows: 95°C for 3 min; 95°C 5 s, 56°C 10 s, 72°C 25 s; 40 cycles. After the reaction, the cycle threshold (Ct) value was obtained. The internal reference was glyceraldehyde-3-phosphate dehydrogenase (GAPDH), and the analytical approach was the  $2^{-\Delta\Delta Ct}$  method. The primer sequences were as follows: *SULF1* forward: 5'-TGGCGAGAATGGCTTGGATTA-3', *SULF1* reverse: 5'-TAACGGGCCTATGGGGATAACA-3'; *GAPDH* forward: 5'-TTGAGGTCAATGAAGGGGTC-3', *GAPDH* reverse: 5'-GAAGGTGAAGTCGGAGTCA-3'.

### Cell Counting Kit-8 (CCK-8) assay

Cells were cultured in 96-well plates (with density of  $3 \times 10^3$  cells per well) until they to be adherent. Next, the plates were collected, and CCK-8 solution (10 μL, BestBio, BB-4202, Shanghai, China) was added to each well. Four hours later, microplate reader (MR-96A, Mindray, Shenzhen, China) was for the detection of optical density value (450 nm).

### 5-Ethynyl-2-deoxyuridine (EdU) assay

Cells inoculated in 96-well plates ( $3 \times 10^3$  cells per well) were placed in an incubator for 24 h. Phosphate buffer saline (PBS)

was rinsed 3 times, and 100  $\mu$ L of 5-Ethynyl-2-deoxyuridine (EdU) staining solution was added to each well. The cells were stained for 2 h under dark condition. Cell fixation, Apollo staining, 4',6-diamidino-2-phenylindole staining (C1005, Beyotime, Shanghai, China), and fluorescence microscopy (Ts2/Ts2-FL, Nikon, Tokyo, Japan) were performed in accordance with the description of the EdU cell proliferation detection kit (Guangzhou RiboBio Co., Ltd., C10310-1, Guangzhou, China). Three fields of view were randomly selected for photographing. Image J software (version 1.4, National Institutes of Health, Bethesda, MD, USA) was for quantitatively analyzing.

### Transwell assay

#### Migration assay

The cells were inoculated in Transwell chambers (Merck, CLS3399, Kenilworth, NJ, USA) at a density  $1 \times 10^5$  cells/well. A complete culture medium was added to the lower 24-well plate. After 24 h of incubation, the medium was discarded. Cells were subjected to PBS washing, 4% formaldehyde fixation for 4 h, and crystal violet solution (Solarbio, C8470, Beijing, China) staining for 10 min. After the upper cells were wiped away, migrating cells were observed under a microscope (DMIL LED, Leica, Wetzlar, Germany). Three fields of view were randomly selected for cell counting.

#### Invasion assay

Before cell inoculation, Transwell chambers supplementing Matrigel (Shanghai Fusheng Industrial Co., Ltd., FS-79064, Shanghai, China) was maintained at 37°C for 30 min. The rest of the procedures were the same as those in the migration experiment.

### Western blot

Radioimmunoprecipitation assay lysis buffer (Merck, 20-188, Kenilworth, NJ, USA) was utilized for total protein extraction. A bicinchoninic acid kit (Merck, BCA1-1KT, Kenilworth, NJ, USA) was used for quantification. Protein (20  $\mu$ g) was added to sodium dodecyl sulfate-polyacrylamide gel electrophoresis (10%) for separation and displaced to polyvinylidene fluoride membranes (Merck, IPFL00010, Kenilworth, NJ, USA). Upon blocking with 5% skimmed milk powder (Solarbio, D8340, Beijing, China), primary antibodies were added to the membranes for overnight incubation at 4°C. The primary antibodies were as follows: E-cadherin (1:1000; A22333) and GAPDH (1:10,000; AC001) purchased from Abclonal (Wuhan, China); N-cadherin (1:1000; 4061), vimentin (1:1000; 3932), c-Jun N-terminal kinase (JNK, 1:1000; 9252), and phospho-JNK (p-JNK, 1:1000; 4671) from CST (Danvers, MA, USA); EGFR (1:5000; 30139-1-AP), phospho-EGFR

(p-EGFR, 1:1000; 30277-1-AP), extracellular signal-regulated kinase (ERK; 1:5000; 51068-1-AP), phospho-ERK (p-ERK; 1:1000; 28733-1-AP), p-p38 MAPK (1:1000; 28796-1-AP), and p38 MAPK (1:1000; 51115-1-AP) from Proteintech (Wuhan, China). Then, the membranes were incubated with goat anti-rabbit immunoglobulin G secondary antibody (1:5000; AS014, Abclonal, Wuhan, China) for 1 h. An enhanced chemiluminescence kit (Thermo Fisher Scientific, WP20005, Waltham, MA, USA) was utilized for exposure development. A Bio-Tanon imaging system (Tanon Science and Technology Co., Ltd., Shanghai, China) was used for visualization, imaging, and quantification. GAPDH was used as the endogenous control, and Image J software was used for quantitative analysis (grayscale analysis).

### Clinical samples

NSCLC tissues and paraneoplastic tissues were obtained from 54 patients with NSCLC who received surgical resection in Ningbo Ninth Hospital from February 2021 to January 2022. NSCLC was diagnosed with computed tomography scan and histopathological biopsy. No preoperative chemotherapy or radiotherapy was administered to a patient before surgery. After cold PBS rinses, the tissues were stored at  $-80^{\circ}\text{C}$ . SULF1 expression in the clinical tissue samples was evaluated using qRT-PCR. The general information of patients was collected, including age, sex, pathological type, differentiation, tumor node metastasis (TNM) stage, and lymph node metastasis. The patients were followed up once a month, and their survival status was recorded. The median follow-up period was 29 months (7–38 months). The ethics committee of Ningbo Ninth Hospital Medical Health Group provided approval (approval number NNHM-20210106). All the procedures complied with the Helsinki Declaration and have obtained informed consent from patients.

### Statistical analysis

The Statistical Package for the Social Sciences 22.0 software (IBM, Armonk, NY, USA) and Graphpad Prism 9.0 (Graphpad, San Diego, CA, USA) were used for statistical analysis and drawing, respectively. The data were presented as mean and standard deviation. Intergroup comparisons were performed using Student's *t*-test (for two groups), and one-way analysis of variance was performed with Tukey's *post hoc* test (for multiple groups). Chi-square test was used for evaluating difference in count data, which was denoted as *n* (%). On the basis of the median SULF1 expression value, the patients were included in the high SULF1 expression group (SULF1 expression above the median) and low SULF1 expression group (SULF1 expression below the median). Difference in overall survival between two groups was evaluated through Kaplan–Meier analysis. The criterion for significant variation was  $P < 0.05$ .

## RESULTS

### Knockdown of SULF1 abated NSCLC cell viability

The Gene Expression Profiling Interactive Analysis (<http://gepia.cancer-pku.cn/>) database indicated that lung adenocarcinoma (LUAD, which is a type of NSCLC) tumor tissues have higher SULF1 expression levels than normal tissues ( $P < 0.05$ ), [Figure 1a]. In contrast to human normal lung epithelial cells BEAS-2B, NSCLC cells showed prominently augmented SULF1 expression levels ( $P < 0.001$ ), [Figure 1b]. Next, si-SULF1 and its negative control were transfected into NCI-H1299 and HCC827 cells. The SULF1 levels in the NSCLC cells were abated after transfected with si-SULF1 relative to those of transfected with si-NC ( $P < 0.001$ ), [Figure 1c and d], which were measured through qRT-PCR. This result indicated that transfection successfully knocked down the SULF1 expression. The results from CCK-8 assay showed that versus the cell viability of si-NC group, the cell viability in si-SULF1 group was prominently abated ( $P < 0.05$ ), [Figure 1e and f]. The EdU-positive cell rates of the NCI-H1299 and HCC827 cells in the si-SULF1 group were considerably lower than the EdU-positive cell rate of the si-NC group ( $P < 0.01$ ), [Figure 1g-j]. The rates were measured with EdU assay. Overall, the knockdown of SULF1 inhibited the activity of the NSCLC cells.

### Knockdown of SULF1 inhibits migration, invasion, and epithelial-to-mesenchymal transition (EMT) in the NSCLC cells

Compared with number of migration and invasion cells of the si-NC group, the number of migration and invasion cells in si-SULF1 group were prominently reduced ( $P < 0.01$ ), [Figure 2a-f]. Epithelial-to-mesenchymal transition (EMT) -related proteins, including the epithelial cell marker E-cadherin and mesenchymal cell markers N-cadherin and vimentin, were evaluated through Western blot. Compared with the si-NC group, the si-SULF1 group exhibited prominently augmented E-cadherin protein level in the H1299 and HCC827 cells ( $P < 0.001$ ) and abated N-cadherin and vimentin protein levels ( $P < 0.01$ ), [Figure 2g-i]. Confirming that SULF1 knockdown repressed the malignant biological behavior of the NSCLC cells, including migration, invasion, and EMT.

### Knockdown of SULF1 abated EGFR/MAPK signaling pathway

p-EGFR/EGFR, p-p38 MAPK/p38 MAPK, p-ERK/ERK, and p-JNK/JNK ratios in the NCI-H1299 and HCC827 cells transfected with si-SULF1 were prominently abated relative to those in the si-NC group ( $P < 0.001$ ), [Figure 3a-j], as indicated by the Western blot results. SULF1 knockdown can abate the EGFR/MAPK signaling pathway.

### EGFR/MAPK signaling pathway mediated the process of SULF1 knockdown suppressing metastasis in NCI-H1299 cell

To further confirm the mechanism of SULF1 in NSCLC cell metastasis, NCI-H1299 cells were handled with the EGFR/MAPK signaling pathway agonist NSC228155. Compared with the si-NC group, the si-SULF1 group showed prominently abated p-EGFR/EGFR, p-ERK/ERK, p-p38 MAPK/p38 MAPK, and p-JNK/JNK. Compared with the si-SULF1 group, the si-SULF1 + NSC228155 group showed considerably augmented p-EGFR/EGFR, p-ERK/ERK, p-p38 MAPK/p38 MAPK, and p-JNK/JNK protein levels in the NCI-H1299 cells ( $P < 0.01$ ), [Figure 4a-c], as indicated by the Western blot results. The results from Transwell assay suggested that versus the si-NC group, the number of the migration and invasion cells of the NCI-H1299 cells in the si-SULF1 group was prominently reduced. Compared with the si-SULF1 group, the si-SULF1 + NSC228155 group showed considerably augmented cell migration and invasion ( $P < 0.05$ ), [Figure 4d and e]. The E-cadherin protein level in the NCI-H1299 cells of the si-SULF1 group greatly increased relative to those in the si-NC group, whereas N-cadherin and vimentin protein levels were abated. The NCI-H1299 cells in the si-SULF1 + NSC228155 group showed abated E-cadherin protein level and considerably increased N-cadherin and vimentin protein levels relative to those in the si-SULF1 group ( $P < 0.05$ ), [Figure 4f and g]. The protein levels were measured with Western blot.

### High SULF1 expression was related to the poor prognosis of patients with NSCLC

To analyze the clinical characteristics of SULF1 and its relationship with the prognoses of NSCLC patients, we collected tumor tissues from 54 patients with NSCLC. A marked increase in SULF1 expression was observed in tumor tissues versus that in adjacent lung tissues ( $P < 0.001$ ), [Figure 5a]. Table 1 displays the general information of 54 patients with NSCLC. No statistically significant difference between the high and low SULF1 expression groups was observed in terms of age, sex, pathological type, differentiation, and lymph node metastasis ( $P > 0.05$ ), but TNM stage presented a significant difference between the two groups ( $P < 0.05$ ), [Table 1]. The median survival times in the high and low SULF1 expression groups were 25 and 31 months, respectively. Furthermore, the overall survival in the high SULF1 expression group was lower than that in the low SULF1 expression group ( $P < 0.05$ ), [Figure 5b], suggesting the poor prognoses of patients with NSCLC and high SULF1 expression levels.

## DISCUSSION

SULF1 is highly expressed in several cancer types and regulates many signals by editing the sulfation modification

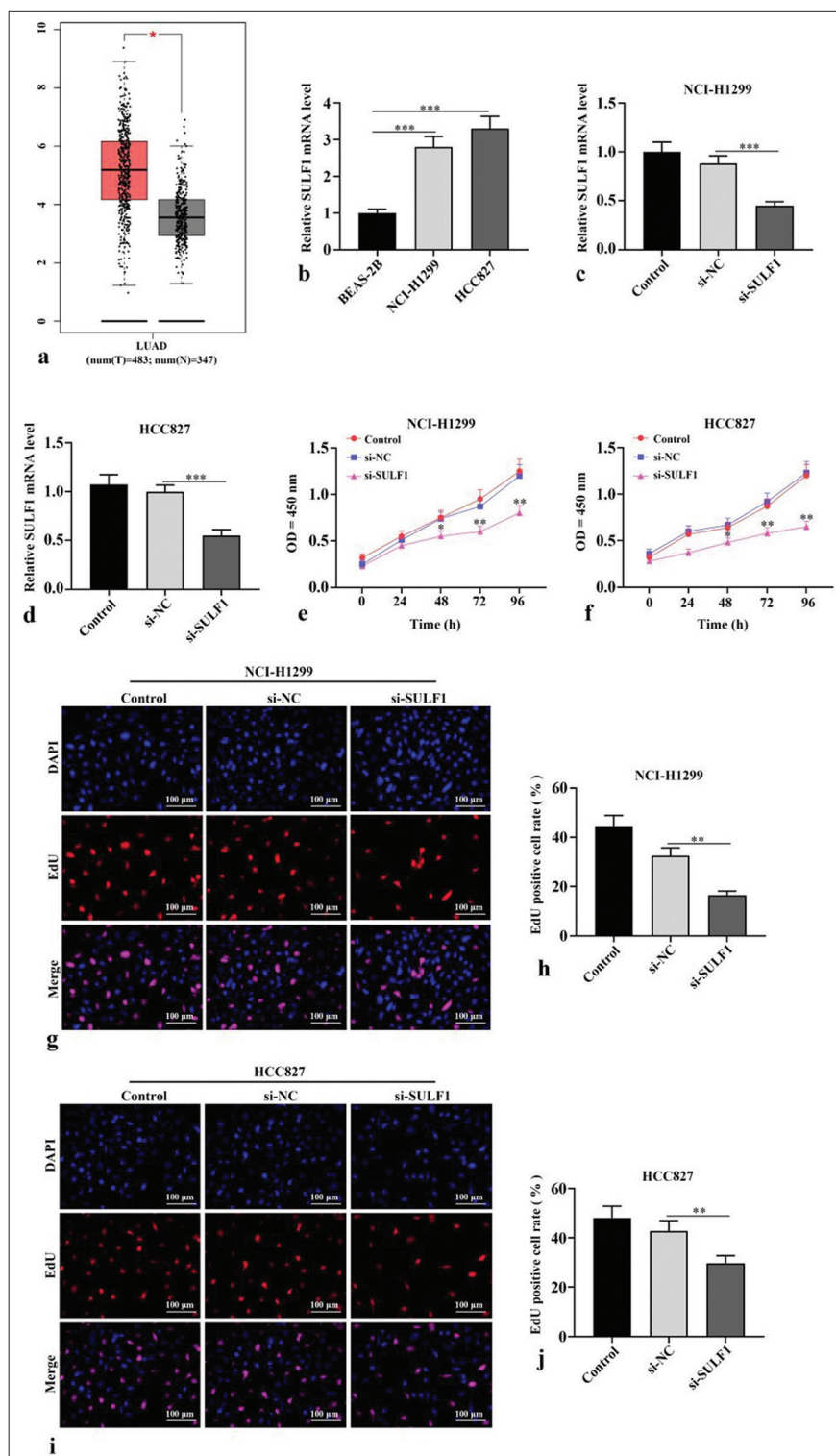


**Figure 1:** Knockdown of SULF1 abated NSCLC cell activity. (a) The gene expression profiling interactive analysis database showed that SULF1 was augmented in the LUAD tissues. The red and gray columns represent the tumor and normal tissues, respectively; (b) SULF1 levels in BEAS-2B, NCI-H1299 and HCC827 evaluated through qRT-PCR,  $n = 3$ ; (c and d) SULF1 levels in cells evaluated through qRT-PCR after the knockdown of SULF1,  $n = 3$ ; (e and f) Cell viability evaluated through CCK-8 assay,  $n = 3$ ; (g-j) EdU positive cell ratio evaluated through EdU experiments,  $n = 3$ . (\* $P < 0.05$ , \*\* $P < 0.01$ , \*\*\* $P < 0.001$ ). (NSCLC: Non-small cell lung cancer, SULF1: Sulfatase 1, LUAD: Lung adenocarcinoma, si-NC: Negative control, si-SULF1: siRNA SULF1, qRT-PCR: Quantitative real-time polymerase chain reaction, CCK-8: Cell counting kit-8, EdU: 5-ethynyl-2-deoxyuridine, OD: Optical density, DAPI: 4',6-diamidino-2-phenylindole).

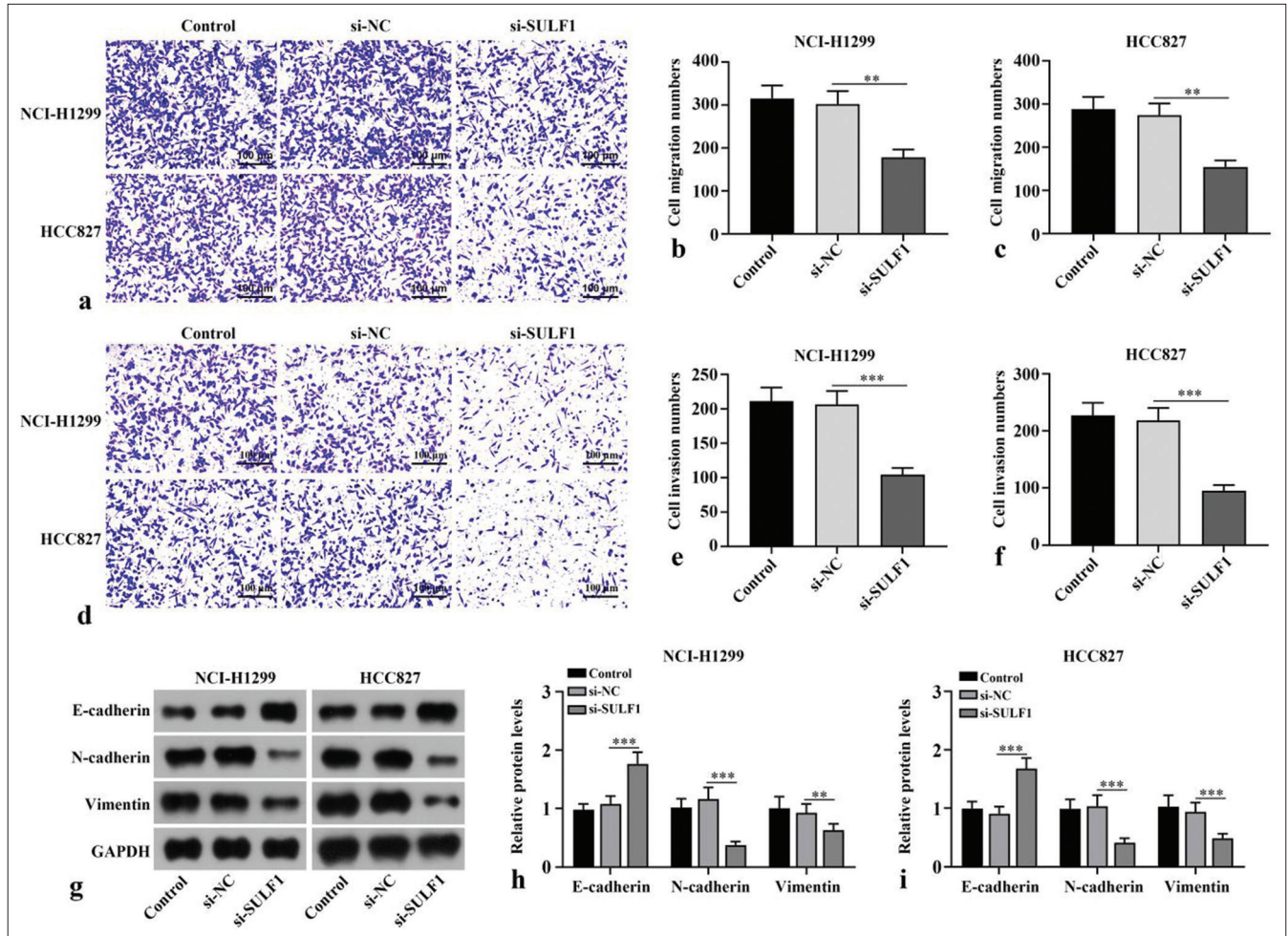


**Figure 2:** Knockdown of SULF1 abated migration, invasion, and EMT in NSCLC cells. (a-f) Cell migration (a-c) and invasion (d-f) measured with Transwell assay,  $n = 3$ . (g-i) EMT-related biomarkers levels detected through Western blot,  $n = 3$ . (\*\* $P < 0.01$ , \*\*\* $P < 0.001$ . NSCLC: Non-small cell lung cancer, SULF1: Sulfatase 1, si-NC: Negative control, si-SULF1: siRNA SULF1, EMT: Epithelial-to-mesenchymal transition).

of heparan sulfate proteoglycans.<sup>[15]</sup> However, understanding of SULF1 in NSCLC and its possible mechanism is lacking. Our study found that SULF1 level was strongly enriched in the NSCLC tissues and cells. Furthermore, patients with NSCLC and high SULF1 expression levels had poor overall survival. The knockdown of SULF1 abated the malignant biological behavior of the NSCLC cells, including proliferation, migration, and invasion.

EMT is an important cellular process that transforms polarized epithelial cells into mesenchymal phenotypes and increases cell motility.<sup>[16]</sup> EMT is abnormally activated under pathological conditions, including organ fibrosis and cancer. During EMT, the epithelial markers level is abated, whereas mesenchymal markers level is augmented.<sup>[17,18]</sup> The inhibition of EMT can help suppress the onset and advancement of NSCLC. Moreover, EMT contributes to chemotherapy and radiotherapy resistance.<sup>[19-21]</sup> The knockdown of SULF1 abated the biological behavior of the NSCLC cells, including

migration, invasion, and EMT. Specifically, it upregulated the E-cadherin level and abated the N-cadherin and vimentin levels. These results indicated that knocking down SULF1 can inhibit the progression of NSCLC by regulating the EMT phenotype.

EGFR is related to a variety of complex cell signal transduction pathways. EGFR forms homodimers or heterodimers by binding to its ligands, thereby activating the PI3K/Akt and MAPK/ERK pathways in cancer.<sup>[22]</sup> In a study of colorectal cancer, the proliferation, migration, and invasion of colorectal cancer cells were promoted by the EGFR/MAPK pathway.<sup>[23]</sup> EGFR/MAPK signaling pathway is engaged in the regulation of malignant behavior in ovarian cancer cells, and blocking this pathway can repress the growth of xenograft tumors.<sup>[24]</sup> A study in lung cancer has shown that inhibiting the EGFR/MAPK pathway can restrain the growth and metastasis of lung cancer cells.<sup>[25]</sup> EGFR/MAPK was also linked to the osimertinib resistance in

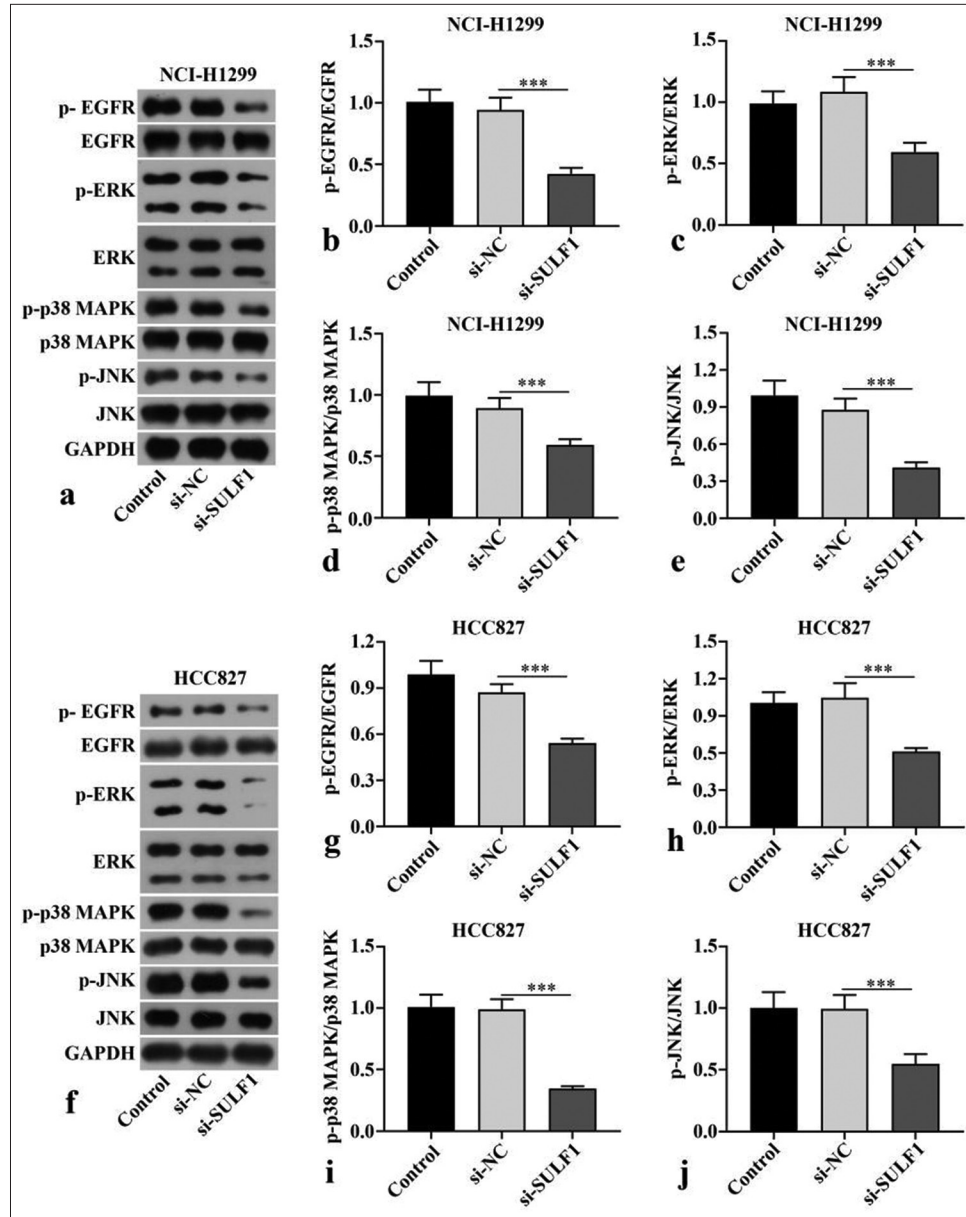


**Figure 3:** Knockdown of SULF1 abated EGFR/MAPK signaling pathway. (a-j) EGFR/MAPK signaling pathway-related proteins levels in the NCI-H1299 (a-e) and HCC827 (f-j) cells evaluated through Western blot,  $n = 3$ . (\*\*\*)  $P < 0.001$ . SULF1: Sulfatase 1, si-NC: Negative control, si-SULF1: siRNA SULF1, EGFR: Epidermal growth factor receptor, p-EGFR: phospho-EGFR, ERK: Extracellular signal-regulated kinase, p-ERK: phospho-ERK, p38 MAPK: p38 mitogen-activated protein kinase, p-p38 MAPK: Phospho-p38 MAPK, JNK: c-Jun N-terminal kinase, p-JNK: Phospho-JNK, GAPDH: Glyceraldehyde-3-phosphate dehydrogenase).

NSCLC.<sup>[26]</sup> In this study, the knockdown of SULF1 reduced p-EGFR/EGFR, p-p38 MAPK/p38 MAPK, p-ERK/ERK, and p-JNK/JNK levels. In addition, NSC228155 partially reversed the suppressive effect of SULF1 knockdown on NSCLC cells, indicating that the suppressive effect of SULF1 knockdown on NSCLC was exerted after the inactivation of the EGFR/MAPK pathway. For the limitations of this

study, the relevant conclusions have not been confirmed through *in vivo* experiments, and the mechanisms of SULF1 and EGFR/MAPK signaling pathways have not been fully determined. Therefore, future studies will further explore the potential mechanism of SULF1 in the progression of NSCLC. In addition, NCI-H1299 and HCC827 were large-cell lung cancer and lung adenocarcinoma cell lines, respectively.

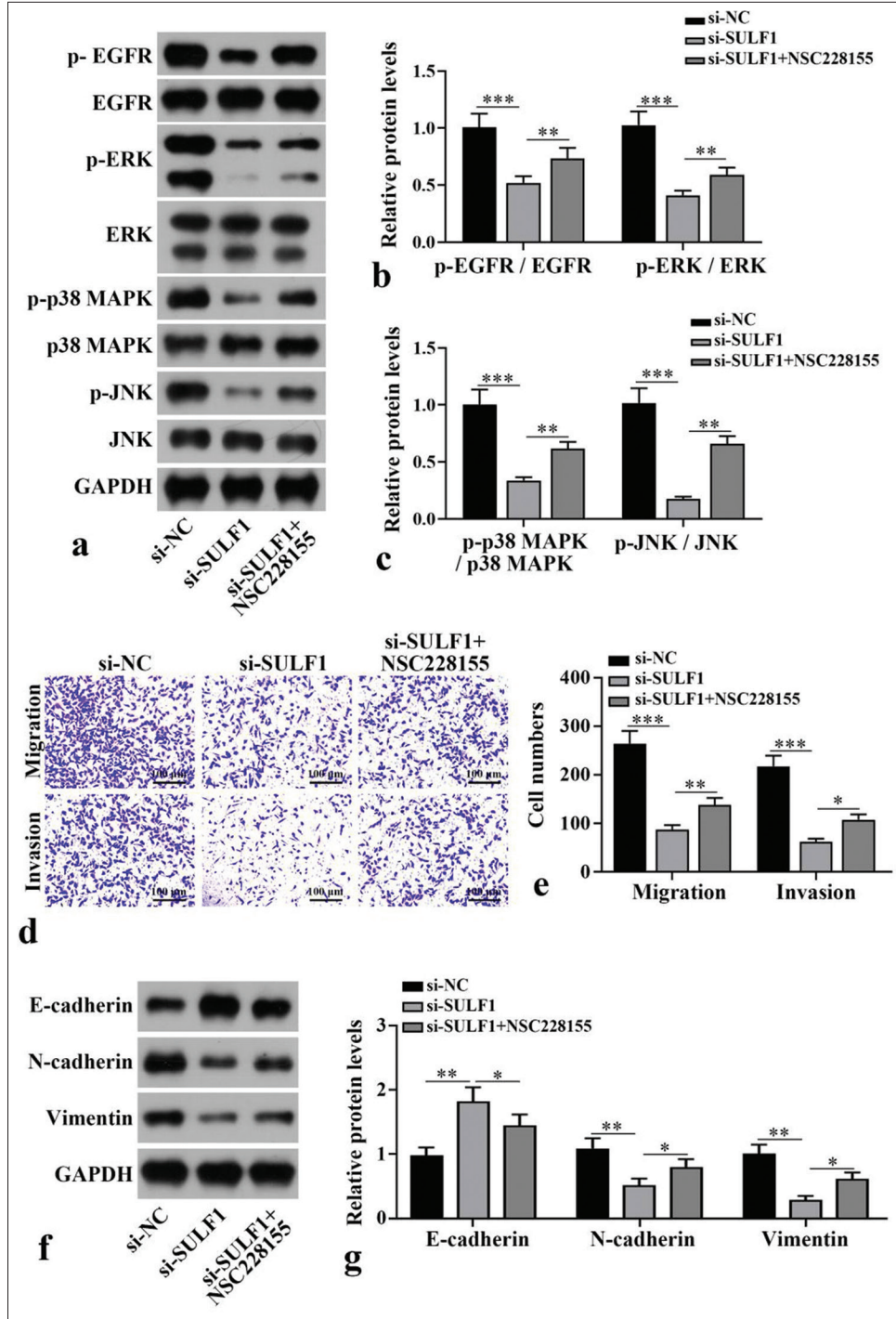


**Figure 4:** EGFR/MAPK signaling pathway mediates the process by which SULF1 promotes NSCLC cell metastasis. NCI-H1299 cells were treated with EGFR agonist NSC228155. (a-c) EGFR/MAPK signaling pathway-related protein levels measured with Western blot,  $n = 3$ . (d and e) Cell migration and invasion levels measured with Transwell assay,  $n = 3$ . (f and g) EMT-related biomarkers levels measured with Western blot,  $n = 3$ . ( $*P < 0.05$ ,  $**P < 0.01$ ,  $***P < 0.001$ . SULF1: Sulfatase 1, si-NC: Negative control, si-SULF1: siRNA SULF1, EGFR: Epidermal growth factor receptor, p-EGFR: Phospho-EGFR, ERK: Extracellular signal-regulated kinase, p-ERK: Phospho-ERK, p38 MAPK: P38 mitogen-activated protein kinase, p-p38 MAPK: Phospho-p38 MAPK, JNK: c-Jun N-terminal kinase, p-JNK: phospho-JNK, GAPDH: Glyceraldehyde-3-phosphate dehydrogenase, EMT: Epithelial-to-mesenchymal transition).



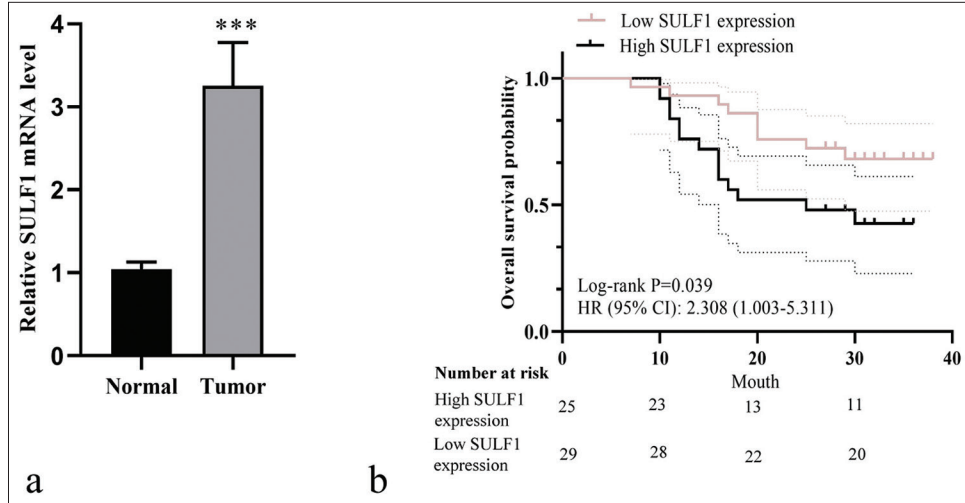


**Figure 5:** High SULF1 expression was related to poor prognosis in patients with NSCLC. (a) SULF1 level detected through qRT-PCR,  $n = 54$ .  $***P < 0.001$ . (b) The Kaplan–Meier curve of high SULF1 expression group ( $n = 25$ ) and low SULF1 expression groups ( $n = 29$ ). (NSCLC: Non-small cell lung cancer, SULF1: Sulfatase 1, HR: Hazard ratio, CI: Confidence interval, qRT-PCR: Quantitative real-time polymerase chain reaction).

**Table 1:** General information of patients with NSCLC.

	NSCLC Patients ( $n=54$ )	SULF1 expression		$\chi^2/t$ -value	P-value
		High SULF1 expression ( $n=25$ )	Low SULF1 expression ( $n=29$ )		
Age (year)	67.92±10.62	69.68±11.58	66.41±9.68	1.13	0.26
Sex ( $n, \%$ )					
Male	34 (63.0)	16 (64.0)	18 (62.1)	0.02	0.88
Female	20 (37.0)	9 (36.0)	11 (37.9)		
Pathological type ( $n, \%$ )					
Adenocarcinoma	30 (55.6)	14 (56.0)	16 (55.2)	0.34	0.84
Large-cell carcinoma	8 (14.8)	3 (12.0)	5 (17.2)		
Squamous cell carcinoma	16 (29.6)	8 (32.0)	8 (27.6)		
TNM stage ( $n, \%$ )					
I–II	25 (46.3)	7 (28.0)	18 (62.1)	6.27	0.01
III	29 (53.7)	18 (72.0)	11 (37.9)		
Differentiation ( $n, \%$ )					
Well and moderate	37 (68.5)	16 (64.0)	21 (72.4)	0.44	0.51
Poor	17 (31.5)	9 (36.0)	8 (27.6)		
Lymph node metastasis ( $n, \%$ )					
Negative	31 (57.4)	14 (56.0)	17 (58.6)	0.04	0.85
Positive	23 (42.6)	11 (44.0)	12 (41.4)		

NSCLC: Non-small cell lung cancer, SULF1: Sulfatase 1, TNM: Tumor node metastasis

Squamous cell carcinoma cell lines, including NCI-H520 and H226, should be investigated as well.

## SUMMARY

This study demonstrated the suppression of SULF1 knocking down on NSCLC. Mechanistically, SULF1 knockdown abated the invasion and metastasis of NSCLC through the EGFR/MAPK signaling pathway, suggesting that SULF1 is a therapeutic target for NSCLC.

## AVAILABILITY OF DATA AND MATERIALS

The data used to support the current finding of this study are available from corresponding author upon request.

## ABBREVIATIONS

NSCLC – Non-small cell lung cancer  
 SULF1 – Sulfatase 1  
 EGFR – Epidermal growth factor receptor  
 MAPK – Mitogen activated protein kinase  
 EMT – Epithelial-to-mesenchymal transition  
 ERK – Extracellular signal-regulated kinase  
 PI3K – Phosphatidylinositol-3-kinase  
 LncRNA – Long non-coding ribonucleic acid  
 siRNA – Small interfering RNA  
 si-SULF1 – siRNA SULF1  
 si-NC – Negative control  
 qRT-PCR – Quantitative real-time polymerase chain reaction  
 GAPDH – Glyceraldehyde-3-phosphate dehydrogenase  
 CCK-8 – Cell Counting Kit-8  
 OD – Optical density  
 EdU – 5-Ethynyl-2-deoxyuridine  
 DAPI – 4',6-diamidino-2-phenylindole  
 JNK – c-Jun N-terminal kinase  
 p-JNK – Phospho-JNK  
 p-EGFR – Phospho-EGFR  
 p-ERK – Phospho-ERK  
 p-p38 MAPK – Phospho-p38 MAPK  
 TNM – Tumor node metastasis  
 PBS – Phosphate buffer saline  
 LUAD – Lung adenocarcinoma  
 HR – Hazard ratio  
 CI – Confidence interval

## AUTHOR CONTRIBUTIONS

TF and BLZ: Designed the research; BLZ, DPL, and LX: Performed the experiments; LX and JC: Analyzed the data. All authors contributed to editorial changes in the manuscript. All authors read and approved the final manuscript. All authors have participated sufficiently in the work and agreed to be accountable for all aspects of the work.

## ETHICS APPROVAL AND CONSENT TO PARTICIPATE

This study was approved by the Ethics Committee of Ningbo Ninth Hospital Medical Health Group (No. NNHM-20210106). Informed consents were obtained from the patients. All procedures complied with the Helsinki Declaration.

## FUNDING

Not applicable.

## CONFLICT OF INTEREST

The authors declare that they have no competing interest.

## EDITORIAL/PEER REVIEW

To ensure the integrity and highest quality of CytoJournal publications, the review process of this manuscript was conducted under a **double-blind model** (authors are blinded for reviewers and vice versa) through an automatic online system.

## REFERENCES

- Xia C, Dong X, Li H, Cao M, Sun D, He S, *et al.* Cancer statistics in China and United States, 2022: Profiles, trends, and determinants. *Chin Med J (Engl)* 2022;135:584-90.
- Chen P, Liu Y, Wen Y, Zhou C. Non-small cell lung cancer in China. *Cancer Commun (Lond)* 2022;42:937-70.
- Li Y, Yan B, He S. Advances and challenges in the treatment of lung cancer. *Biomed Pharmacother* 2023;169:115891.
- Deshpand R, Chandra M, Rauthan A. Evolving trends in lung cancer: Epidemiology, diagnosis, and management. *Indian J Cancer* 2022;59:S90-105.
- Kim HY, Kim HS. Sulfatase 1 mediates IL-10-induced dimethylarginine dimethylaminohydrolase-1 expression and antiproliferative effects in vascular smooth muscle cells of spontaneously hypertensive rats. *Cytokine* 2021;137:155344.
- Li J, Wang X, Li Z, Li M, Zheng X, Zheng D, *et al.* SULF1 activates the VEGFR2/PI3K/AKT pathway to promote the development of cervical cancer. *Curr Cancer Drug Targets* 2024;24:820-34.
- Yang Y, Ahn J, Edwards NJ, Benicky J, Rozeboom AM, Davidson B, *et al.* Extracellular heparan 6-O-endosulfatases SULF1 and SULF2 in head and neck squamous cell carcinoma and other malignancies. *Cancers (Basel)* 2022;14:5553.
- Sigismund S, Avanzato D, Lanzetti L. Emerging functions of the EGFR in cancer. *Mol Oncol* 2018;12:3.
- Ayati A, Moghimi S, Salarinejad S, Safavi M, Pouramiri B, Foroumadi A. A review on progression of epidermal growth factor receptor (EGFR) inhibitors as an efficient approach in cancer targeted therapy. *Bioorg Chem* 2020;99:103811.
- Herbst RS, Wu YL, John T, Grohe C, Majem M, Wang J, *et al.* Adjuvant osimertinib for resected EGFR-mutated stage IB-IIIa

- non-small-cell lung cancer: Updated results from the phase III randomized ADAURA trial. *J Clin Oncol* 2023;41:1830-40.
11. He J, Huang Z, Han L, Gong Y, Xie C. Mechanisms and management of 3<sup>rd</sup> generation EGFR-TKI resistance in advanced non-small cell lung cancer (review). *Int J Oncol* 2021;59:90.
  12. Xu H, Yang X, Xuan X, Wu D, Zhang J, Xu X, *et al.* STAMPB promotes lung adenocarcinoma metastasis by regulating the EGFR/MAPK signaling pathway. *Neoplasia* 2021;23:607-23.
  13. Acheampong F, Ostlund T, Mahnashi M, Halaweish F. Estrone analogs as potential inhibitors targeting EGFR-MAPK pathway in non-small-cell lung cancer. *Chem Biol Drug Des* 2023;101:1356-66.
  14. Chen LM, Niu YD, Xiao M, Li XJ, Lin H. LncRNA NEAT1 regulated cell proliferation, invasion, migration and apoptosis by targeting has-miR-376b-3p/SULF1 axis in non-small cell lung cancer. *Eur Rev Med Pharmacol Sci* 2020;24:4810-21.
  15. Yang YW, Phillips JJ, Jablons DM, Lemjabbar-Alaoui H. Development of novel monoclonal antibodies and immunoassays for sensitive and specific detection of SULF1 endosulfatase. *Biochim Biophys Acta Gen Subj* 2021;1865:129802.
  16. Leggett SE, Hruska AM, Guo M, Wong IY. The epithelial-mesenchymal transition and the cytoskeleton in bioengineered systems. *Cell Commun Signal* 2021;19:32.
  17. Lu W, Kang Y. Epithelial-mesenchymal plasticity in cancer progression and metastasis. *Dev Cell* 2019;49:361-74.
  18. Fan Q, Liang X, Xu Z, Li S, Han S, Xiao Y, *et al.* Pedunculoside inhibits epithelial-mesenchymal transition and overcomes Gefitinib-resistant non-small cell lung cancer through regulating MAPK and Nrf2 pathways. *Phytomedicine* 2023;116:154884.
  19. Yang X, Jiang H, Ning J, Zhang S, Cai Y, Wang L, *et al.* Inhibition of GPR30 sensitized gefitinib to NSCLC cells via regulation of epithelial-mesenchymal transition. *Int J Immunopathol Pharmacol* 2023;37:1-9.
  20. Ji H, Zhang L, Zou M, Sun Y, Dong X, Mi Z, *et al.* SPATA2 suppresses epithelial-mesenchymal transition to inhibit metastasis and radiotherapy sensitivity in non-small cell lung cancer via impairing DVL1/ $\beta$ -catenin signaling. *Thorac Cancer* 2023;14:969-82.
  21. Hu X, Jiang C, Hu N, Hong S. ADAMTS1 induces epithelial-mesenchymal transition pathway in non-small cell lung cancer by regulating TGF- $\beta$ . *Aging (Albany NY)* 2023;15:2097-114.
  22. Jiang W, Wang X, Zhang C, Xue L, Yang L. Expression and clinical significance of MAPK and EGFR in triple-negative breast cancer. *Oncol Lett* 2020;19:1842-8.
  23. Tang R, Chen J, Tang M, Liao Z, Zhou L, Jiang J, *et al.* LncRNA SLCO4A1-AS1 predicts poor prognosis and promotes proliferation and metastasis via the EGFR/MAPK pathway in colorectal cancer. *Int J Biol Sci* 2019;15:2885-96.
  24. Ji J, Li C, Wang J, Wang L, Huang H, Li Y, *et al.* Hsa\_circ\_0001756 promotes ovarian cancer progression through regulating IGF2BP2-mediated RAB5A expression and the EGFR/MAPK signaling pathway. *Cell Cycle* 2022;21:685-96.
  25. Yin Y, Xie J, Peng F, Tan L, Xiao Y, Zheng H, *et al.* The topoisomerase inhibitor CPT-11 prevents the growth and metastasis of lung cancer cells in nude mice by inhibiting EGFR/MAPK signaling pathway. *Heliyon* 2023;9:e15805.
  26. Ning Y, Zheng H, Yang Y, Zang H, Wang W, Zhan Y, *et al.* YAP1 synergize with YY1 transcriptional co-repress DUSP1 to induce osimertinib resistant by activating the EGFR/MAPK pathway and abrogating autophagy in non-small cell lung cancer. *Int J Biol Sci* 2023;19:2458-74.

**How to cite this article:** Zhang B, Luo D, Xiang L, Chen J, Fang T. Investigating the anti-cancer potential of sulfatase 1 and its underlying mechanism in non-small cell lung cancer. *CytoJournal*. 2024;21:52. doi: 10.25259/Cytojournal\_71\_2024

HTML of this article is available FREE at:  
[https://dx.doi.org/10.25259/Cytojournal\\_71\\_2024](https://dx.doi.org/10.25259/Cytojournal_71_2024)

The FIRST **Open Access** cytopathology journal

Publish in *CytoJournal* and **RETAIN** your copyright for your intellectual property

**Become Cytopathology Foundation (CF) Member at nominal annual membership cost**

For details visit <https://cytojournal.com/cf-member>

PubMed indexed

**FREE** world wide **open access**

**Online processing** with rapid turnaround time.

**Real time** dissemination of time-sensitive technology.

Publishes as many **colored high-resolution images**

Read it, cite it, bookmark it, use RSS feed, & many----



**CYTOJOURNAL**

[www.cytojournal.com](http://www.cytojournal.com)

Peer-reviewed academic cytopathology journal





# NextGen CelBloking™ Kits

**Frustrated with your cell blocks?  
We have a better solution!**

**Nano**

## Nano NextGen CelBloking™

Cell block kit to process single scattered cell specimens and tissue fragments of **any** cellularity.



**PATENT PENDING**



**Pack #1**



**Pack #2**

**Micro**

## Micro NextGen CelBloking™

For cellular specimens (more than 1 ml concentrated specimen with Tissuecrit more than 50%)



**PATENT PENDING**



**Pack #1**



**Pack #2**